Structure and microstructure of the ferromagnetic superconductor $RuSr_2GdCu_2O_8$

A. C. McLaughlin, W. Zhou, and J. P. Attfield
Interdisciplinary Research Centre in Superconductivity, University of Cambridge, Madingley Road, Cambridge CB3 0HE United Kingdom
and Department of Chemistry, University of Cambridge, Lensfield Road, Cambridge CB2 1EW, United Kingdom

A. N. Fitch
European Synchrotron Radiation Facility, Boîte Postale 220, 38043 Grenoble Cedex, France

J. L. Tallon
Industrial Research Limited, P.O. Box 13130, Lower Hutt, New Zealand
(Received 19 April 1999)

Two samples of $RuSr_2GdCu_2O_8$, in which ferromagnetism and superconductivity coexist at low temperatures, have been studied by high-resolution electron microscopy and synchrotron x-ray-diffraction methods. The average crystal structure is tetragonal at both 10 and 295 K, but a superstructure resulting from coherent rotations of the RuO_6 octahedra within subdomains of 50–200 Å are observed by electron diffraction. The Cu-O bond distances indicate a high hole concentration ($p \approx 0.4$) in the CuO_2 planes, which is inconsistent with the previously observed underdoped transport properties ($p \approx 0.1$). This may reflect extensive hole trapping by the Ru moments. [S0163-1829(99)02834-9]

INTRODUCTION

Coexisting ferromagnetism and superconductivity have recently been discovered in the 1212-type layered cuprate $RuSr_2GdCu_2O_8$.[1] This material displays a Curie transition at $T_M = 132$ K and bulk superconductivity below $T_c = 0-46$ K depending on sample preparations. A variety of physical measurements, in particular, zero-field muon spin rotation experiments,[2] have demonstrated that the material is microscopically uniform with no evidence for spatial phase separation of superconducting and magnetic regions. Superconductivity appears to be associated with the copper oxide planes while the ruthenium oxide slab behaves like $SrRuO_3$,[3] which is an itinerant electron ferromagnet below $T_M = 165$ K, rather than Sr_2RuO_4, which is a *p*-wave superconductor with $T_c \approx 1$ K.[4,5]

The above and previous studies of $RuSr_2GdCu_2O_8$ (Refs. 6 and 7) have shown that the physical properties are strongly dependent on sample preparation conditions. Long annealing times are needed to suppress the formation of $SrRuO_3$ and achieve the ferromagnetic superconducting phase. In this study we have characterized the structure and microstructure of two $RuSr_2GdCu_2O_8$ samples using high-resolution synchrotron x-ray powder diffraction and electron microscopy. Although neutron diffraction is the method of choice for magnetic oxides, the high absorption cross section of natural Gd for thermal neutrons makes the technique impractical here without isotopic enrichment.

EXPERIMENT

$RuSr_2GdCu_2O_8$ was synthesized by a solid-state reaction of stoichiometric powders of RuO_2, $SrCO_3$, Gd_2O_3, and CuO. These were decomposed at 960 °C in air then ground, milled, and die-pressed into pellets before preliminary reaction in flowing nitrogen at 1010 °C for 10 h followed by reaction in flowing oxygen at 1050 °C and 1055 °C for 10 h each. The sample was furnace cooled, reground, and repelleted between each step. Part of the latter ''as-prepared'' sample was heated at 1060 °C in flowing oxygen for 7 days and slow cooled to room temperature, giving the ''annealed'' sample. Thermogravometric analysis of the annealed sample under flowing hydrogen/nitrogen gave an oxygen content of 8.00 ± 0.02, and another analysis 3 months later gave 7.99 ± 0.03.

Selected area electron diffraction (SAED) patterns and high-resolution transmission electron microscopic (HRTEM) images were recorded from the as-prepared and annealed $RuSr_2GdCu_2O_8$ samples on a JEOL JEM-200CX electron microscope. Each sample was powdered and dispersed on a copper grid covered by a holey carbon film. The spherical and chromatic aberration coefficients of $C_s = 0.41$ mm and $C_c = 0.95$ mm, respectively, give an interpretable resolution of ~1.85 Å.

Powder synchrotron x-ray-diffraction patterns of the annealed sample were recorded on ESRF beam line BM16 at 10 and 295 K.[8] The sample was contained in a 0.5-mm-diameter borosilicate glass capillary mounted on the axis of the diffractometer about which it was spun at ~1 Hz to improve the powder averaging of the crystallites. For the low-temperature measurement, the capillary was spun inside a liquid-helium-cooled flow cryostat. To minimize absorption, relatively short wavelengths of 0.309 65(5) and 0.321 03(5) Å were used at 10 and 295 K, respectively. Diffraction patterns were collected over the angular ranges 2–62° (10 K) and 2–40° (295 K) by continuously scanning the bank of nine Ge (111) analyzer crystals and scintillation detectors at a rate of 0.5 deg/min, and recording the data every 200 ms. The high-angle parts of the pattern were scanned several times to improve the statistical quality of the data in these regions. The counts from the nine detectors of the various scans were normalized, summed, rebinned to a constant step size of 0.004°, and then fitted using the GSAS program.[9]

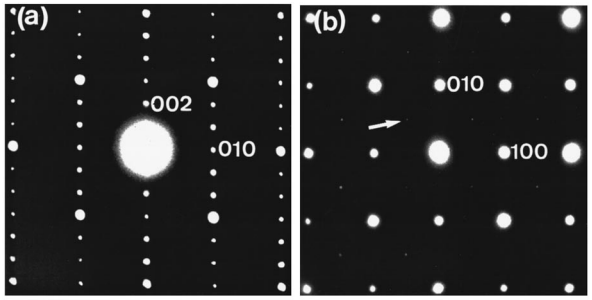

FIG. 1. SAED patterns from the as-prepared $RuSr_2GdCu_2O_8$, viewed down (a) the [100] and (b) the [001] directions. The main diffraction spots are indexed by the basic tetragonal unit cell with $a \approx 3.84$ and $c \approx 11.6$ Å. The additional weak spots arrowed in (b) evidence the $\sqrt{2}a \times \sqrt{2}a \times c$ superstructure.

RESULTS

Transport and magnetic measurements of the as-prepared and annealed $RuSr_2GdCu_2O_8$ samples have been reported elsewhere.[1] The as-prepared material has $T_c(R=0)=20$ K and $T_M=132$ K. Annealing raises $T_c(R=0)$ to 37 K but the ferromagnetic transition is almost unchanged with $T_M=134$ K.

All of the main diffraction spots in the SAED patterns (Fig. 1) from the as-prepared specimen can be indexed by the basic tetragonal unit cell expected for 1212-type cuprates with $a \approx 3.84$ and $c \approx 11.6$ Å. However, additional weak spots on the SAED pattern viewed down the [001] direction [Fig. 1(b)] indicate that a $\sqrt{2}a \times \sqrt{2}a \times c$ supercell is formed. When large areas of this sample were examined, each particle was found to contain many domains. A typical HRTEM image is shown in Fig. 2. The areas labeled *A*, *B*, and *C* are individual domains. *A* and *C* are both oriented in the [100] direction, but rotated by 90° from one another. Domain *B* ([001] orientation) is perfectly intergrown between *A* and *C* without any amorphous boundaries. Area *D* shows an intergrowth of *A* and *B* with an interface on the (100) planes for both domains. The intergrowth of *A* and *B* in the area *E* is between the (010) plane of *A* and the (001) plane of *B*.

The SAED patterns from microcrystallites of the annealed specimen are similar to those from the as-prepared material and show the $\sqrt{2}a \times \sqrt{2}a \times c$ supercell. However, the domain microstructure is significantly changed by the annealing process, as shown by the HRTEM image in Fig. 3 that is projected on the [001] zone axis. No irregular domain boundaries are observed and the underlying structure is coherent across the area of the image, however, some unusual rectangular boundaries are observed.

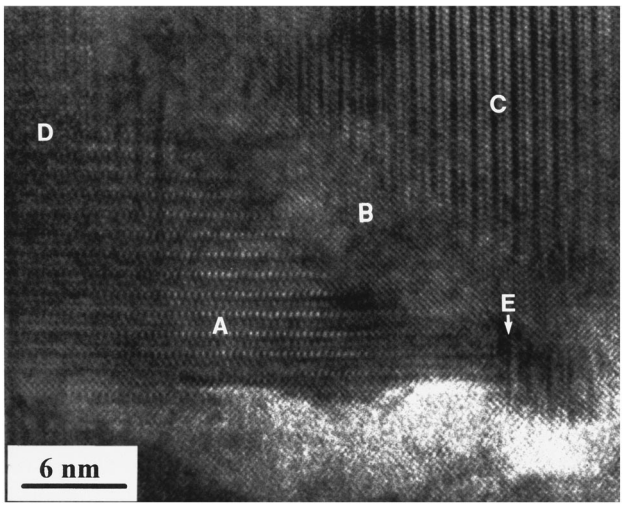

FIG. 2. HRTEM image of a region of as-prepared $RuSr_2GdCu_2O_8$, showing multidomain structures. The marked areas are described in the text.

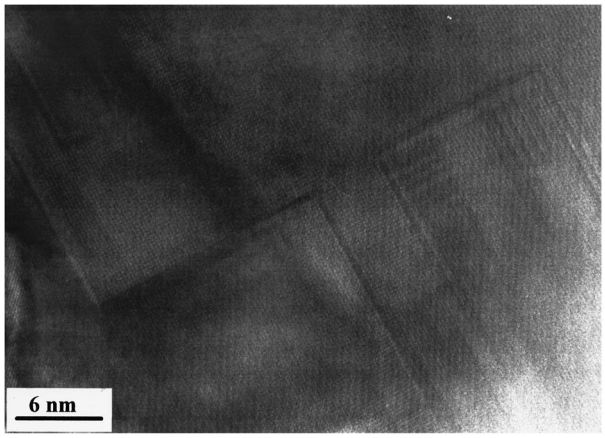

FIG. 3. HRTEM image of the annealed $RuSr_2GdCu_2O_8$ sample viewed down the [001] zone axis showing rectangular antiphase boundaries.

Synchrotron x-ray diffraction shows the annealed sample to be highly crystalline with peakwidths (full-width at half-maximum) ~0.03° 2θ. In the 295 K data, the maximum peak intensity is 22 000 counts against a background of 50 counts. This gives a very high sensitivity to weak diffraction peaks, however, no reflections from the supercell found by electron microscopy or from secondary phases such as $SrRuO_3$ were seen. All of the observed peaks can be indexed on the tetragonal $a \times a \times c$ cell.

An excellent Rietveld fit to the 295 K profile was obtained with a tetragonal, $P4/mmm$ symmetry structural model (Table I) and no evidence for an orthorhombic distortion was observed. The atomic displacement *U* factors for all the sites could be refined anisotropically except for Ru, which gave one negative principal *U* value, and was subsequently refined isotropically. Disorder of the oxygen atoms within the RuO_2 planes, O(3), and of the apical oxygen atoms O(1) linking the CuO_5 units and RuO_6 octahedra was evidenced by large *U* values. This was modeled by using a single isotropic *U* factor for all the oxygen atoms and splitting the sites as shown in Table I. The disorder of O(1) is fitted with [100] displacements, although we cannot exclude alternative directions such as [110]. The metal site occupancies refined to within ±1% of full occupancy showing that no significant cross substitutions are present. Refining the oxygen site occupancies did not yield any significant deviations from complete filling, although neutron diffraction is needed for a precise determination.

The 10 K synchrotron diffraction pattern of the annealed $RuSr_2GdCu_2O_8$ sample (Fig. 4) is similar to the 295 K profile, although background scatter from the cryostat resulted in some regions of the profile being excluded from the Rietveld fit. The previous structural model (Table I) gives an excellent fit to the data, with group isotropic displacement parameters being used for the metal atoms and oxygens.

TABLE I. Refined cell parameters, agreement factors, and atomic parameters for $RuSr_2GdCu_2O_8$ at 10 and 295 K (upper and, where different, lower values, respectively).

T (K)	a (Å)	c (Å)	Volume (Å^3)	R_{wp}	R_p	χ^2		
10	3.8303 2(3)	11.5494(1)	169.444(3)	0.083	0.065	5.9		
295	3.8384 1(2)	11.5731(1)	170.511(3)	0.074	0.059	4.9		
Atom	Site	x	y	z	U_{iso} (Å^2)[a]	U_{11} (Å^2)[b]	U_{33} (Å^2)[b]	Occupancy
Ru	1(b)	0	0	0.5	0.000 10(2)			1.00
					0.001 7(2)			
Sr	2(h)	0.5	0.5	0.308 77(6)	0.000 10			1.00
				0.308 95(7)	0.006 1(2)	0.0064(2)	0.0057(3)	
Gd	1(c)	0.5	0.5	0.0	0.000 10			1.00
					0.001 2(2)	0.0015(2)	0.0006(3)	
Cu	2(g)	0	0	0.144 77(8)	0.000 10			1.00
				0.145 27(10)	0.003 5(3)	0.0014(2)	0.0058(4)	
O(1)	8(s)	0.051(3)	0	0.333 6(5)	0.003 1(5)			0.25
		0.039(4)		0.333 5(5)	0.008 6(6)			
O(2)	4(i)	0	0.5	0.129 5(3)	0.003 1			1.00
				0.130 6(3)	0.008 6			
O(3)	4(o)	0.122(2)	0.5	0.5	0.003 1			0.50
		0.114(2)			0.008 6			

[a]Refined isotropic thermal parameters except for the anisotropically refined atoms in which case the equivalent isotropic value is given.

[b]All the anisotropically refined sites have $U_{11}=U_{22}\neq U_{33}$, $U_{12}=U_{13}=U_{23}=0$.

DISCUSSION

The average structure of $RuSr_2GdCu_2O_8$ (Fig. 5) is similar to that of other 1212-type cuprate superconductors, and consists of a layer of almost regular RuO_6 octahedra connected through their apices to two layers of CuO_5 square pyramids. Several features in the crystal structure are important in determining the microstructure observed by electron microscopy. The c/a axis ratio of 3.015 (at 295 K) is very close to the ideal value for a triple perovskite structure. For comparison, c/a varies between 3.032 and 3.066 as δ changes from 0 to 1 in $YBa_2Cu_3O_{7-\delta}$.[10] The near coincidence of a and b with $c/3$ in $RuSr_2GdCu_2O_8$ results in the formation of many small domains with c in one of three almost equivalent directions, as observed in the micrograph in Fig. 2. The 90° angle between the CuO_2 planes meeting at the boundaries between these domains strongly reduces the supercurrent transport leading to granularity, a low transport T_c and a high residual resistivity in the as-prepared $RuSr_2GdCu_2O_8$ sample.[1] The improvement in superconducting properties following the long high-temperature anneal is thus a microstructural effect due to increases in domain size (Fig. 3), rather than a simple change in cation composition or oxygen content. This is confirmed by subsequent heat-capacity studies that show that the thermodynamic transition occurs at $T_c=46$ K in both samples.[11] The ferromagnetic order within the RuO_2 planes appears to be insensitive to these domain effects.

The mismatch between lengths of the in-plane Ru-O and Cu-O bonds results in rotations of the RuO_6 octahedra around c by 13° at 295 K. A slight tilting of the polyhedra that reduces the Cu-O-Ru angle to 173° is also observed. These displacements are not significantly different at 10 K,

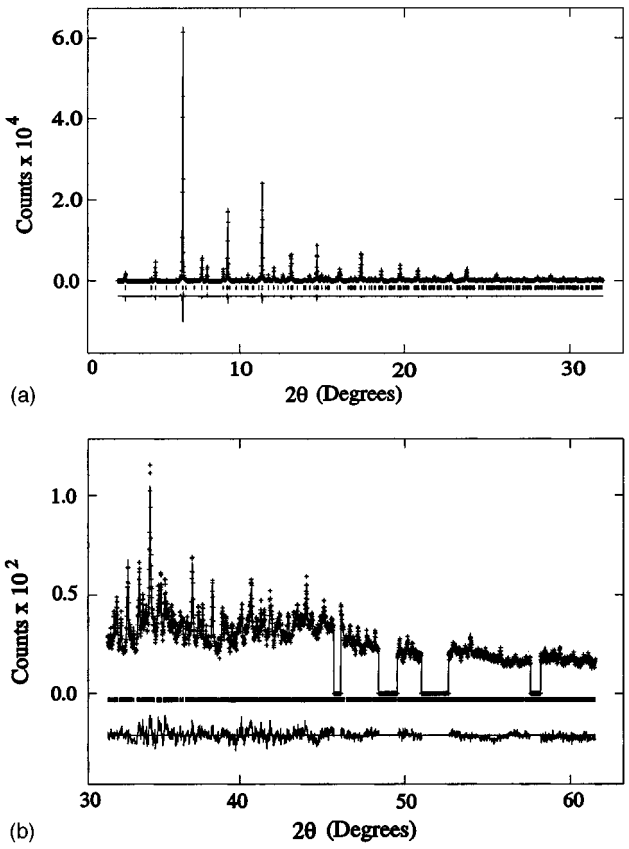

FIG. 4. Observed, calculated, and difference synchrotron x-ray-diffraction data for the annealed $RuSr_2GdCu_2O_8$ sample at 10 K. Excluded regions at high angles contain additional scattering from the cryostat.

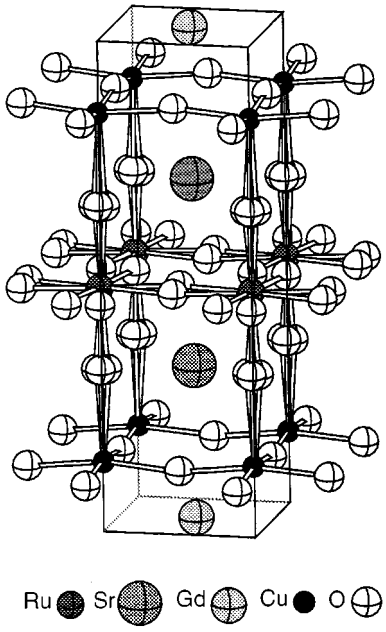

FIG. 5. The average crystal structure of $RuSr_2GdCu_2O_8$ showing the disordered rotations of the RuO_6 octahedra.

showing that they are due to static disorder within the average structure rather than phonon motion. The rotations of the RuO_6 octahedra would give rise to a $\sqrt{2}a\times\sqrt{2}a\times c$ superstructure if long-range ordered (Fig. 6), which is observed by electron diffraction (Fig. 1) but not in the x-ray diffraction patterns. This is consistent with the presence of many antiphase boundaries of width a at which the sense of rotation of the RuO_6 octahedra around c is reversed but the remainder of the structure is unaffected (Fig. 6). These are observed as the dark rectangular boundaries in the HRTEM of the annealed sample (Fig. 3) and divide the structure into subdomains of 50–200 Å, which are sufficiently large for the superstructure to be seen by electron diffraction but too short to give rise to observable superstructure peaks in the x-ray data.

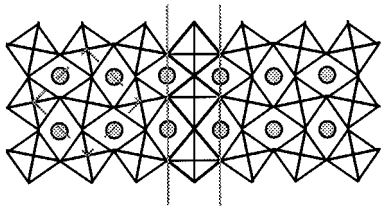

FIG. 6. A model for the rotations of the RuO_6 octahedra around c in the $RuSr_2GdCu_2O_8$ structure, resulting in a $\sqrt{2}a\times\sqrt{2}a$ superstructure in the xy plane shown by broken lines. An antiphase boundary within which local distortions of the RuO_6 octahedra occur is also shown. This reverses the sense of rotation of the octahedra.

There is no evidence for cation disorder or oxygen nonstoichiometry in the annealed $RuSr_2GdCu_2O_8$ sample on the basis of our diffraction and thermogravimetric measurements. Hence, the formal oxidation states of Cu and Ru may be written as $2+p$ and $5-2p$, respectively, where p is the amount of charge transferred between the CuO_2 and RuO_2 planes. In the lower limit of $p=0$, both the CuO_2 and RuO_2 planes would be antiferromagnetically ordered and insulating due to the Hubbard splitting of the Cu $d_{x^2-y^2}$ band, as observed in undoped cuprates, and the t_{2g}^3 configuration of Ru^{5+}, as found in Sr_2YRuO_6.[12] Charge transfer introduces p holes into the $d_{x^2-y^2}$ subband of the CuO_2 planes and $2p$ electrons into the minority spin t_{2g} band of the RuO_2 layers. For the upper limit of $p=0.5$, both the CuO_2 and the RuO_2 layers would be expected to have itinerant electron behavior; the former layers would be too overdoped to superconduct,

TABLE II. Interatomic distances (Å) and angles (°) in $RuSr_2GdCu_2O_8$ at 10 and 295 K (upper and lower values, respectively). The ranges given for some angles reflect the static disorder of the O(1) site.

Distance (Å)			Angle (°)
Cu-O(1)×1	2.189(6)	O(1)-Cu-O(2)	90.1–100.4(3)
	2.184(6)		91.1–99.0(4)
Cu-O(2)×4	1.9232(3)	O(2)-Cu-O(2)	89.52(2)
	1.9268(4)		89.55(2)
Ru-O(1)×2	1.932(6)	O(2)-Cu-O(2)	169.5(2)
	1.933(5)		169.9(2)
Ru-O(3)×4	1.971(2)	O(1)-Ru-O(1)	180
	1.969(2)		180
Gd-O(2)×8	2.430(2)	O(1)-Ru-O(3)	84.4–95.6(3)
	2.443(2)		85.6–94.4(4)
Sr-O(1)×2	2.590(7)	O(3)-Ru-O(3)	90
	2.625(9)		90
Sr-O(1)×2	2.865(8)	O(3)-Ru-O(3)	180
	2.838(10)		180
Sr-O(2)×4	2.820(3)	Cu-O(1)-Ru	169.1(6)
	2.819(3)		171.5(8)
Sr-O(3)×2	2.641(4)	Cu-O(2)-Cu	169.5(2)
	2.661(4)		169.9(2)
Sr-O(3)×2	3.249(5)	Ru-O(3)-Ru	152.6(4)
	3.232(5)		154.3(4)

but the latter can give rise to ferromagnetic order as found in $SrRuO_3$.[2,13]

The observed superconductivity and ferromagnetism in $RuSr_2GdCu_2O_8$ shows that p lies between the above extremes. p may be estimated from the structural data using bond valence summations that make use of the sensitivity of Cu-O bond lengths to the hole concentration.[14] In $RuSr_2GdCu_2O_8$, the four in-plane Cu-O(2) distances are comparable to those in other cuprate superconductors, but the 2.19 Å apical Cu-O(1) bond is unusually short compared, e.g., to 2.30 Å in $YBa_2Cu_3O_7$ (Ref. 9) and 2.35 Å in overdoped $TlSr_2CaCu_2O_{7-\delta}$ (Ref. 15). This results in a high value of $p \approx 0.4$, calculated using the 295 K bond lengths distances in Table II, and the method of Ref. 16.

The estimate of $p \approx 0.4$ appears to be inconsistent with the observed superconductivity in this $RuSr_2GdCu_2O_8$ sample, and with the previous estimate of $p \approx 0.1$ (i.e., underdoped superconductivity) based on transport measurements.[1] This contradiction suggests that a large proportion of the holes is trapped by defects or by the ferromagnetic order in the sample. The principal interaction between the carriers in the CuO_2 planes and the Ru moments, in the absence of a direct exchange, is a classical electromagnetic one. This vanishes if both the carrier momentum and the field are parallel to the xy plane, and therefore predicts that the Ru moments lie in this plane (otherwise the pairbreaking would be too severe for superconductivity to occur). However, a slight canting of the moments may arise due to a Dzyaloshinsky-Moriya interaction between neighboring Ru moments, which is nonzero due to the rotations and tilts of the RuO_6 octahedra. This can lead to magnetic trapping or scattering of the holes and hence transport properties typical of nonmagnetic underdoped cuprates, while the total hole concentration measured crystallographically is much higher.

CONCLUSIONS

$RuSr_2GdCu_2O_8$ has a tetragonal 1212-type structure typical of many cuprates, but with an unprecedented short apical Cu-O bond of 2.19 Å. No gross structural changes occur on cooling from 295 to 10 K, below the ferromagnetic and superconducting transitions at 132 and 37 K, respectively. Although this material is cation and oxygen stoichiometric, disorder in the average structure and microstructure arises from the c/a ratio being very close to 3, and from the mismatch between Cu-O and Ru-O distances within their respective MO_2 planes. The former coincidence results in many small misoriented domains in as-prepared samples, and long high-temperature annealing is needed to produce large domain material. The bond length mismatch leads to rotations of the RuO_6 octahedra around c, and the formation of subdomains separated by sharp antiphase boundaries at which the sense of rotation is reversed. The hole doping of the CuO_2 planes required for superconductivity results from overlap of the Cu $d_{x^2-y^2}$ and Ru t_{2g} bands. The measured bond distances indicate that a high degree of charge transfer occurs, but this is at odds with reported transport properties that are characteristic of underdoped cuprates. This may reflect a magnetic hole-trapping interaction and further experiments are needed to clarify this issue.

ACKNOWLEDGMENTS

We thank EPSRC for the provision of research Grant No. GR/M59976, ESRF beam time, and support for A.C.M. J.L.T. acknowledges support under a Royal Society of New Zealand James Cook Fellowship and from the Marsden Fund.

[1] J. L. Tallon, C. Bernard, M. E. Bowden, T. M. Stoto, B. Walker, P. W. Gilberd, M. R. Presland, J. P. Attfield, A. C. McLaughlin, and A. N. Fitch (unpublished).

[2] C. Bernhard, J. L. Tallon, Ch. Niedermayer, Th. Blasius, A. Golnik, E. Brucher, R. K. Kremer, D. R. Noakes, C. E. Stronach, and E. J. Ansaldo, Phys. Rev. B **59**, 14 099 (1999).

[3] J. M. Longo, P. M. Raccah, and J. B. Goodenough, J. Appl. Phys. **39**, 1327 (1968).

[4] Y. Maeno, H. Hashimoto, K. Yoshida, S. Nishizaki, T. Fujita, J. G. Bednorz, and F. Lichtenberg, Nature (London) **372**, 532 (1994).

[5] K. Ishida, H. Mukuda, Y. Kitaoka, K. Asayama, Z. Q. Mao, Y. Mori, and Y. Maeno, Nature (London) **396**, 658 (1998).

[6] L. Bauernfeind, W. Widder, and H. F. Braun, Physica C **254**, 151 (1995).

[7] I. Felner, U. Asaf, S. Reich, and Y. Tsabba, Physica C **311**, 163 (1999).

[8] A. N. Fitch, in *European Powder Diffraction Conference: EPDIC IV*, edited by R. J. Cernik, R. Delhez, and E. J. Mittemeijer [Mater. Sci. Forum **228-231,** 219 (1996)]; J. L. Hodeau, P. Bordet, M. Anne. A. Prat, A. N. Fitch, E. Dooryhee, G. Vaughan, and A. Freund, Proc. SPIE **3448**, 353 (1998).

[9] A. C. Larson and R. B. Von Dreele, Los Alamos National Laboratory Report No. LA-UR-86-748, 1994 (unpublished).

[10] a is taken to be the geometric mean of a and b for orthorhombic compositions. Data were taken from D. C. Johnston *et al.*, in *Chemistry of High Temperature Superconductors*, edited by D. L. Nelson, M. S. Whittingham, and T. F. George, ACS Symp. Ser. 351 (American Chemical Society, Washington, DC, 1987), p. 136.

[11] J. L. Tallon, J. W. Loram, G. V. M. Williams, and C. Bernhard (unpublished).

[12] P. D. Battle and W. J. Maclin, J. Solid State Chem. **54**, 245 (1984).

[13] J. H. Cho, Q. X. Jia, X. D. Wu, S. R. Foltyn, and M. P. Maley, Phys. Rev. B **54**, 37 (1996).

[14] I. D. Brown, J. Solid State Chem. **82**, 122 (1989).

[15] Y. Shimakawa, J. D. Jorgensen, B. A. Hunter, H. Shaked, R. L. Hitterman, Y. Kubo, T. Kondo, T. Manako, H. Takahashi, and N. Mori, Physica C **253**, 71 (1995).

[16] J. L. Tallon, Physica C **168**, 85 (1990); **176**, 547 (1995).